

Capacity Evaluation of an Indoor Smart Antenna System at 60 GHz

Nektarios Moraitis¹ and Demosthenes Vouyioukas²

¹Mobile Radiocommunications Laboratory, National Technical University of Athens

9 Heroon Polytechniou str. 15773, Zografou, Athens, Greece
morai@mobile.ntua.gr

²Dept. of Information and Communication Systems Engineering, University of the Aegean
Karlovasi 83200 Samos, Greece
dvouyiou@aegean.gr

Abstract. In this paper, a study for indoor channel modeling is presented for the millimeter frequency band, by using various configurations of multiple element antenna systems. A multi-ray model is proposed and verified through simulation process for capacity prediction of a high data rate wireless system. The proposed model utilizes the geometric characteristics of the environment, the angle of arrival and angle of departure of each one of the propagation paths, the antenna elements and their spacing. The results showed that the system capacity increases significantly if two or four elements are used at both terminal antennas instead of the basic SISO configuration. In order to accomplish major improvement in the data rates, a MIMO system at 60 GHz should operate within a range of 10 to 20 m in an indoor environment with the view of obtaining sufficient Signal to Noise Ratios.

1 Introduction

Multiple antenna systems and in general multiple input-multiple output (MIMO) systems are an optimistic technique for future wireless communications, valuable for overcoming the effects of multipath interference and thus giving capacity and spectrum efficiency. Over the last years, the force for wireless systems and in particular for mobile communications to deal with new services requires high capacity, robustness against interferences, privacy and accurate prediction of the reception signals, thus modeling of the propagation channel. The demand for data rates greater than 2 Mb/s up to 155 Mb/s are enormous and Wireless Broadband Systems (WBSs) are emerging rapidly.

Please use the following format when citing this chapter:

Moraitis, Nektarios, Vouyioukas, Demosthenes, 2006, in IFIP International Federation for Information Processing, Volume 204, Artificial Intelligence Applications and Innovations, eds. Maglogiannis, I., Karpouzis, K., Bramer, M., (Boston: Springer), pp. 271–280

In millimeter wave frequencies the propagation modeling, apart from the known empirical models, can be realized based on geometrical optics using ray-tracing theory. In the 60 GHz region the diffraction phenomenon can be neglected, and the sum of the direct ray and the reflected rays is enough to describe the behavior of the propagation channel with great accuracy [1]. The modeling in extremely high frequencies poses the problem of the accurate description of the propagation scenarios at the wavelength scale (5 mm at 60 GHz). Hence the main target is to describe the main obstructions and the surfaces that affect the signal propagation. The description is not only in terms of the geometric characteristics of the propagation environment, but also in terms of the surface electromagnetic parameters (relative dielectric constant, losses etc) in order to extract the surface reflection coefficients.

In this paper we present a multi-ray model in order to describe the signal propagation at 60 GHz in an indoor environment and to calculate further the capacity of the proposed MIMO system. In order to predict the performance of multiple array systems, the angle of arrival and angle of departure of each one of the propagation paths, jointly with the antenna elements and their spacing, were considered. The presented channel model is based on the assumption, that there are few dominant reflections of the signal - four single reflected plus four double reflected rays plus the direct component - consisting of a total of 9 rays. The propagation mechanisms are explained analytically whereas channel parameters, such as propagation paths and the corresponding gains of each path arriving at the receive antenna, are calculated.

This paper is organized as follows; section 2 deals with the channel modeling and the proposed multi-ray model and explaining the mechanisms and the behavior of the signal propagation. In Section 3 an analytically description of the geometry of the environment under consideration is presented along with the simulation procedure of the proposed channel model, dealing with two different geometry scenarios. In Section 4, the results of the space-time channel model are presented taking into consideration the accomplishment of the capacity improvement ($C > 1$ b/s/Hz), in order to evaluate the total throughput of the MIMO system. Finally, Section 5 is devoted to discussion and conclusions derived by the entire simulation procedure.

2 Channel Model

In order to calculate the capacity of a system with one antenna element at both terminals, the channel impulse response, $h(\tau)$, between the transmit and receive antenna is a prerequisite. In case of a multiple input-multiple output (MIMO) configuration, which has N_{TX} transmit antennas and M_{RX} receive antennas the channel matrix has to be calculated [2]. The $N_{TX} \times M_{RX}$ channel matrix $H(\tau)$ for a MIMO system denotes the impulse response $h_{ij}(\tau)$, between the j -th ($j = 1, 2, \dots, N_{TX}$) transmit antenna and the i -th ($i = 1, 2, \dots, M_{RX}$) receive antenna. One of the most widely used physical models to calculate the channel matrix $H(\tau)$ is [3]:

$$H(\tau) = \sum_{l=1}^L \beta_l a_R(\phi_{R,l}, \theta_{R,l}) a_T^*(\phi_{T,l}, \theta_{T,l}) \quad (1)$$

where L is the number of propagation paths, β_l are the corresponding gains of each path arriving at the receive antenna, $\phi_{R,l}$ and $\theta_{R,l}$ are the azimuth and elevation angles of a propagation path arriving at the receiver antenna, whereas $\phi_{T,l}$ and $\theta_{T,l}$ are the azimuth and elevation angles of a path departing from the transmit antenna. The symbol $*$ denotes conjugate transpose. Furthermore, $a_R(\phi_R, \theta_R)$ is the array response vector for a plane wave arriving from direction ϕ_R , θ_R and $a_T(\phi_T, \theta_T)$ represents the transmitter steering vector for the direction ϕ_T , θ_T . The model given by (1) is based on the assumption that there are few spatially well separated dominant reflectors in the far-field. For each dominant reflector one significant multipath is assumed. In the case of uniform linear arrays (ULAs) with spacing Δx at both transmitter and receiver antennas, and the elements placed along the x-axis of the propagation plane (shown in Fig. 1), the array steering and response vectors are given by:

$$a_T(\phi_T, \theta_T) = \begin{bmatrix} 1 & e^{-j\frac{2\pi}{\lambda}\Delta x \cos(\phi_T) \sin(\theta_T)} & \dots & e^{-j\frac{2\pi}{\lambda}\Delta x(N_{TX}-1) \cos(\phi_T) \sin(\theta_T)} \end{bmatrix}^T \quad (2a)$$

$$a_R(\phi_R, \theta_R) = \begin{bmatrix} 1 & e^{-j\frac{2\pi}{\lambda}\Delta x \cos(\phi_R) \sin(\theta_R)} & \dots & e^{-j\frac{2\pi}{\lambda}\Delta x(M_{RX}-1) \cos(\phi_R) \sin(\theta_R)} \end{bmatrix}^T \quad (2b)$$

where t denotes transpose, N_{TX} and M_{RX} are the number of the elements at the transmit and receive antenna respectively and λ is the wavelength (5 mm at 60 GHz). Equation (1) has also a matrix representation and is given by [3]:

$$H(\tau) = A_R(\phi_R, \theta_R) H_P A_T^*(\phi_T, \theta_T) \quad (3)$$

where $A_R(\phi_R, \theta_R)$ is an $M_{RX} \times L$, and $A_T(\phi_T, \theta_T)$ is an $N_{TX} \times L$ matrix respectively and both are given by:

$$A_R(\phi_R, \theta_R) = \begin{bmatrix} a_R(\phi_{R,1}, \theta_{R,1}) & a_R(\phi_{R,2}, \theta_{R,2}) & \dots & a_R(\phi_{R,L}, \theta_{R,L}) \end{bmatrix} \quad (4a)$$

$$A_T(\phi_T, \theta_T) = \begin{bmatrix} a_T(\phi_{T,1}, \theta_{T,1}) & a_T(\phi_{T,2}, \theta_{T,2}) & \dots & a_T(\phi_{T,L}, \theta_{T,L}) \end{bmatrix} \quad (4b)$$

where L is the number of propagation paths. In (3) $H_P = \text{diag}(\beta_1, \beta_2, \dots, \beta_L)$ is a $L \times L$ matrix that contains the gain of the each propagation path. Hence by using (3) we can calculate the $N_{TX} \times M_{RX}$ channel matrix $H(\tau)$, if we know the angle of arrival (AoA) and angle of departure (AoD) of each one of the L propagation paths, the antenna elements and their spacing. The power gains β_l (received amplitude) of each path can be calculated by using a multi-ray model which describes the signal propagation at a desired frequency.

The multi-ray model is a general case of the two-ray model for more than two reflected components. The reflected components may exhibit single or double reflection from a plane surface. The reflection geometry can be described in the

horizontal as well as in the vertical plane as shown in Fig. 1. Hence, if we know the geometry of the environment where the signal propagates (length, width, height) and the surface reflection coefficients, the received power of each reflected ray could be determined as well as the AoAs and AoDs of each ray. The total received power can be calculated by the summation of N single reflected and M double reflected rays given by [4], [5]:

$$\beta = \sqrt{K} \left| \frac{1}{d_0} + \sum_{i=1}^N \frac{R_i}{d_i} e^{j\Delta\phi_i} + \sum_{j=1}^M \frac{R_{j_a} \cdot R_{j_b}}{d_j} e^{j\Delta\phi_j} \right| \quad (5)$$

where d is the horizontal separation between the transmitter and receiver, d_0 is the path length of the direct component and d_i , d_j are the path lengths each of the i single and j double reflected rays. Moreover, R_i is the reflection coefficient of i single reflected ray whereas R_{j_a} , R_{j_b} are the reflection coefficients of the j double reflected rays on a and b reflecting surfaces respectively. Finally $\Delta\phi_i = 2\pi\Delta l_i / \lambda$ and $\Delta\phi_j = 2\pi\Delta l_j / \lambda$ are the phase differentials between the direct and the reflected rays with Δl_i and Δl_j the differential path lengths between the direct and the i single and j double reflected rays, and λ is the wavelength. The factor K is a constant that incorporates the transmitted power, antenna gains etc. From (5) the total received power β at a given distance d between the transmitter and receiver can be calculated. The power of each one of the reflected arrays β_i can be easily calculated and the total number of paths $L=M+N+1$. Hence, knowing the path gains the AoDs and the AoAs of the reflected rays from (5), we can determine the $N_{TX} \times M_{RX}$ channel matrix $H(\tau)$ by substituting (2a), (2b), (4a) and (4b) in (3).

Finally after calculating the channel matrix of a $N_{TX} \times M_{RX}$ system, its capacity, assuming a channel unknown to the transmitter, can be easily obtained as a function of the signal to noise ratio (SNR), according to the relationship [2]:

$$C = \log_2 \det \left(I_{M_{RX}} + \frac{E_s}{N_{TX} N_0} HH^* \right) \quad (6)$$

where $I_{M_{RX}}$ is a unitary $M_{RX} \times M_{RX}$ matrix, E_s / N_0 is the SNR, N_{TX} stands for the transmitter antenna elements and $*$ denotes conjugate transpose. The capacity is referred as the error free spectral efficiency, or the data rate per unit bandwidth that can be sustained reliably over the MIMO link. Thus given a bandwidth W Hz, the maximum achievable data rate over this bandwidth using the MIMO channel will be WC b/s.

3 Simulation Procedure

The simulation environment is a corridor with dimensions $30 \times 1.75 \times 2.80$ m³ as shown in Fig. 1. The left and right wall surface is made of brick and plasterboard with wooden doors every 3 m but in order to simplify the simulation procedure we assume the surface as a uniform wall, made of brick and plasterboard with its dielectric characteristics given in Fig. 1. The floor is made of concrete and covered with marble, whereas the suspended ceiling is made of aluminium sheets, holding the

fluorescent light tubes. Furthermore, all the material characteristics are provided as well as the propagation geometry and the terminal positions. Each terminal it is assumed to have one, two or four elements with Δx spacing orientated along the x-axis of the propagation plane as illustrated in Fig. 1.

In order to simplify the simulation procedure and reduce the calculation time we use in (5) four single reflected ($N=4$), plus four double reflected ($M=4$) rays plus the direct component (9 reflected rays in total). Hence, H_P will be a 9×9 matrix, $A_R(\phi_R, \theta_R)$, a $M_{RX} \times 9$ matrix, and $A_T(\phi_T, \theta_T)$, a $N_{TX} \times 9$ matrix respectively.

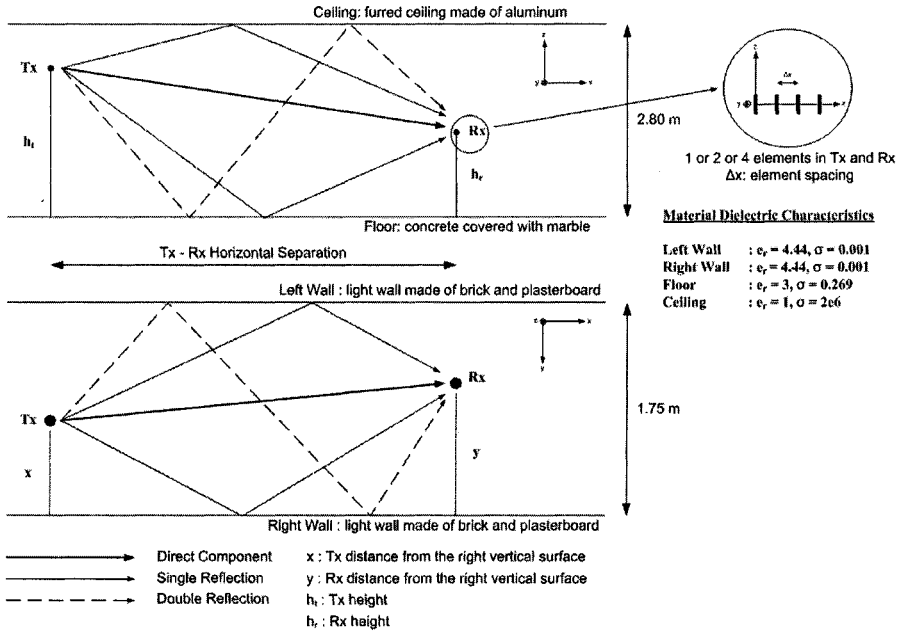


Fig. 1. Simulation environment, propagation geometry and material dielectric characteristics.

Some additional assumptions are:

- The diffraction is not taken into account, since at 60 GHz the phenomenon is almost negligible and the diffracted power does not contribute to the total received power.
- The non-uniformities of the surface materials in indoor environments are such that the produced scattering has not a substantial contribution to the received power.
- The most significant contribution is from the 9 rays previously reported. Further reflected rays are not taken into account since their contribution to the total received power is insignificant. It has been shown [4], [5] that 9 rays in total can describe with great accuracy the signal propagation in the specific environment.
- Only second order reflections are taken into account, since third or fourth order reflections, especially at 60 GHz, are negligible contributors to the average power.

- Atmospheric propagation losses are not taken into account since in indoor environments the attenuation is very small (11.6 dB/km) [6].

During the entire simulation procedure vertical polarization is assumed. Hence, for the rays reflected from vertical walls we use the perpendicular reflection coefficient (R_{\perp}), whereas for the rays from floor and ceiling surfaces we use the parallel reflection coefficient (R_{\parallel}). Both reflection coefficients are given in [7]. In the reflection coefficient equations the complex dielectric constant [7] is given by $\epsilon = \epsilon_r - j60\sigma\lambda$ where ϵ_r is the relative dielectric constant of the reflecting surface, σ is the conductivity of the surface in Siemens/m and λ is the wavelength. The values of ϵ_r and σ are given in Fig. 1 [8], [9].

We consider two different scenarios regarding the terminal positions at the propagation environment. At the first scenario (S1) we assume $h_t = 1.5$ m, $h_r = 1.35$ m, $x = 1.25$ m and $y = 0.5$ m. At the second scenario (S2) the inputs are $h_t = 2.5$ m, $h_r = 1.5$ m, $x = 0.875$ m (center of the corridor) and $y = 0.5$ m. At both scenarios the element spacing Δx in (2a) and (2b) is taken 2λ or 1 cm. Furthermore, at each scenario we considered three different antenna configurations; one element at both terminals (SISO system), two elements at both terminals (2×2 , MIMO system), and four elements at both terminal antennas (4×4 MIMO system).

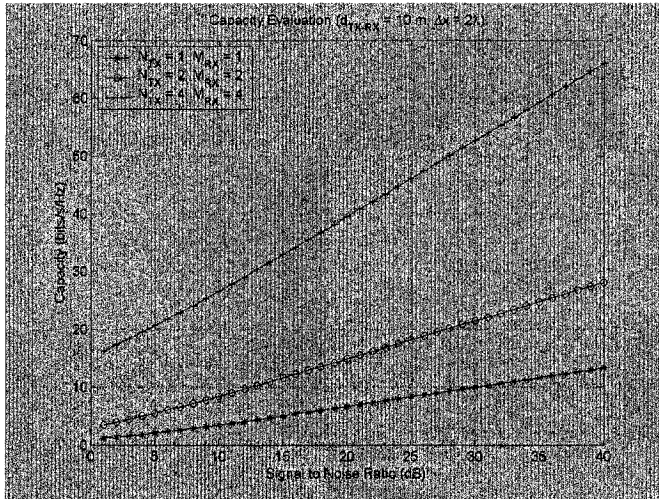
Finally, the simulation is conducted with MatLab script, using 9 rays in total. The channel matrix described by (3) was calculated for each predetermined scenario and for the three different antenna configurations. Then substituting the channel matrix $H(\tau)$ in (6), the capacity of the channel in b/s/Hz was calculated as a function of the desired signal to noise ratio.

4 Results

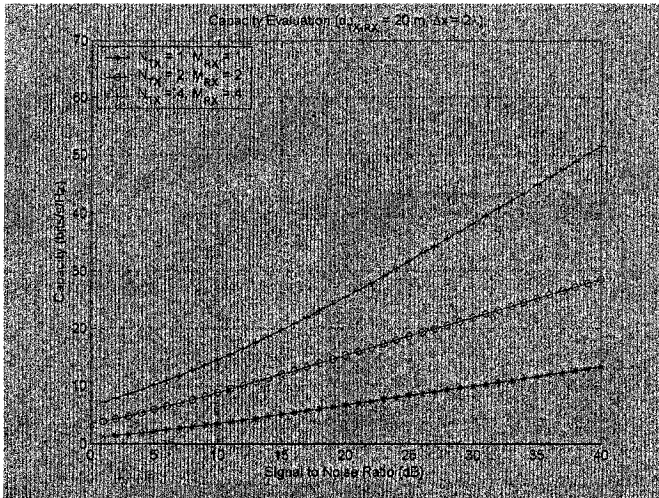
For an efficient system that operates with more than one element antennas, is required to fulfill $C > 1$ b/s per unit bandwidth. Fig. 2 presents the capacity for a 60 GHz system as a function of the SNR derived by the aforementioned simulation procedure. The first scenario has been considered (S1), whereas the distance between the transmitter and receiver has been selected 10 m and 20 m. It is clear that the capacity increases if the antenna elements are increased for a given value of SNR. For example if we select 10 dB SNR and 10 m distance, the capacity increases from 3.5 b/s/Hz for a SISO system to 8.4 b/s/Hz for a 2×2 MIMO and up to 26.6 b/s/Hz for a 4×4 MIMO system. In other words by using four elements at both terminals we can almost multiply by eight the data rate per unit bandwidth relative to SISO system at the frequency of 60 GHz. If we increase the distance (20 m) from Fig. 2b we observe that for a 10 dB SNR the capacity is 3.5 b/s/Hz for a SISO system, 8.8 b/s/Hz for a 2×2 MIMO and 14.6 b/s/Hz for a 4×4 MIMO system. The efficiency of the system is lower at greater distances since the propagation losses at 60 GHz are significant.

Fig. 3 presents the capacity for a 60 GHz system as a function of the SNR for the second scenario (S2). For a 10 m distance, and a 4×4 MIMO system with 10 dB SNR the capacity drops from 26.6 b/s/Hz to 14.6 b/s/Hz. In average, the capacity

increases 3.4 b/s/Hz if we lower the transmitter, regarding all the antenna configurations.



(a)

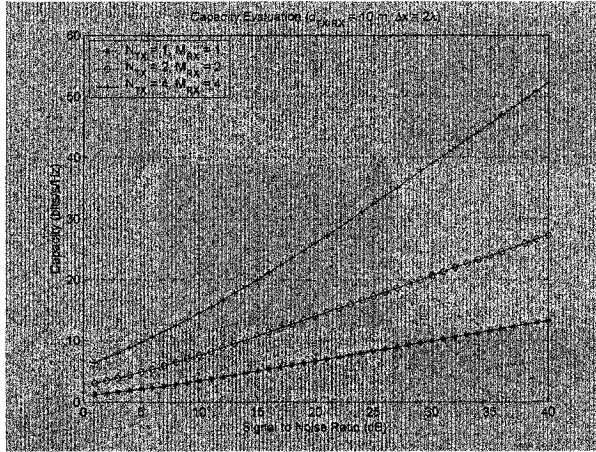


(b)

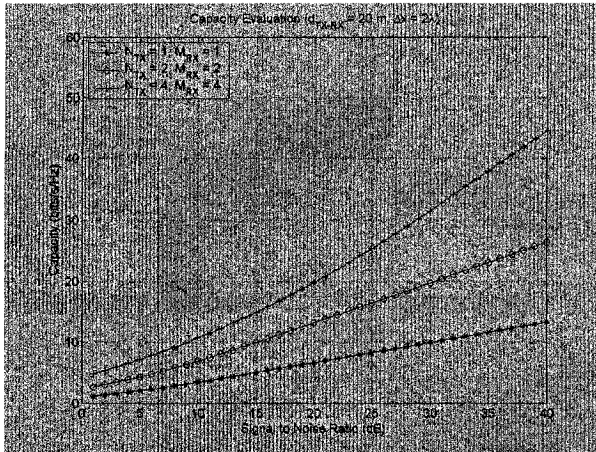
Fig. 2. Capacity as a function of SNR for the first scenario (S1) and two different distances between the transmitter and receiver, (a) 10 m and (b) 20 m

According to [10] the systems that operate at 60 GHz will be a part of fourth generation systems (4G) and may feature transmission rates up to 155 Mb/s especially in an indoor environment. In Europe two frequency segments having a

bandwidth of 1 GHz have been allocated around 60 GHz. This will give the capability to allocate channels up to 100 MHz for the users [11].



(a)



(b)

Fig. 3. Capacity evaluation as a function of SNR for the second scenario (S2) and two different distances between the transmitter and receiver, (a) 10 m and (b) 20 m.

According to this, having a 100 MHz bandwidth available and combining the results derived by the simulation procedure, we can achieve an explicit transmission rate of 2.7 Gb/s for a 4×4 MIMO system with 10 dB SNR at a distance of 10 m from the transmitter for the first scenario (S1). For a 20 m distance the rate will be 1.5 Gb/s. For the second scenario (S2) the achievable rates are 1.5 Gb/s at 10 m and 1.1 Gb/s at 20 m from the transmitter respectively. It is evident that in order to

realize a major improvement in the data rates, a MIMO system at 60 GHz should operate within a range of 10 to 20 m maintaining low SNR (10 dB at least in order to double the data rate per unit bandwidth relative to SISO system).

In [12] wideband channel measurements were performed in the same corridor, transmitting a bandwidth of 100 MHz. The results revealed that the channel exhibits frequency selective characteristics. The coherence bandwidth that determines the performance of a digital system was found 22.48 MHz for 90% correlation and 54.11 MHz for 75% correlation respectively. This is the useful bandwidth that one can achieve the maximum potential data rate without coding (22.48 Mb/s or 54.11 Mb/s). Based on this if we apply a 4×4 MIMO system with 10 dB SNR at a distance of 10 m from the transmitter for the second scenario (S2), the feasible rates will be 327 Mb/s (for 90% correlation) and 788 Mb/s (for 75% correlation). The data rate is increased significantly. For a 20 m distance the rates become 241 Mb/s and 581 Mb/s respectively.

5 Conclusions

This paper presented a simulation procedure in an indoor environment at 60 GHz in order to evaluate the capacity by using multiple element antennas. Different scenarios were evaluated and compared. It was found, that the system capacity increases significantly if two or four elements are used at both terminal antennas instead of the basic SISO configuration. Furthermore, it was observed that in order to realize a major improvement in the data rates, a MIMO system at 60 GHz should operate within a range of 10 to 20 m with the view of maintaining low Signal to Noise Ratios. Efficient capacities, that would at least double the data rates per unit bandwidth relative to a SISO system, can be obtained while the volume of SNR maintaining equal and over 10 dB.

The main target as a future work is to extent the channel model and thus the simulation procedure in different environment types, applying different antenna configurations. Also, SIMO and MISO configurations will be investigated, incorporating different element number, positions and spacing.

References

1. Correia L.M, Prasad R., An overview of wireless broadband communications, *IEEE Commun. Mag.* (1997) 28-33.
2. Paulraj A., Nabar R., Gore D., Introduction to space-time wireless communications, Cambridge University Press (2003).
3. Sayeed A. M., Modeling and Capacity of Realistic Spatial MIMO Channels, *IEEE Int. Conf. on Acoustics, Speech, and Sig. Proc.*, Vol.4 (2001) 2489-2492.
4. Moraitis N., Constantinou P.: Indoor channel modeling at 60 GHz for wireless LAN applications, *Proc. PIMRC '02*, Vol. 3 (2002) 1203-1207.
5. Moraitis N., Indoor radio channel characterization at millimeter wave frequencies for the development of wireless broadband systems, Ph.D. thesis, National Technical University of Athens (2004).

6. Moraitis N., P. Constantinou, Indoor channel measurements and characterization at 60 GHz for wireless local area network applications, *IEEE Trans. on Antennas and Propagation*, Vol. 52 no. 12 (2004) 3180-3189.
7. Rappaport T.S., *Wireless Communications*, Upper Saddle River, NJ: Prentice Hall (1996).
8. Sato K. et al, Measurements of the complex refractive index of concrete at 57.5 GHz, *IEEE Trans. Antennas Propagation*, Vol. 44 no. 1 (1996) 35-39.
9. Sato K. et al., Measurements of reflection and transmission characteristics of interior structures of office building in the 60-GHz band, *IEEE Trans. Antennas Propagation.*, Vol. 45 no. 12 (1997) 1783-1792.
10. Smulders P., Exploiting the 60 GHz band for local wireless multimedia access: prospects and future directions, *IEEE Commun. Mag.*, Vol. 40 no. 1 (2002) 140-147.
11. Prasad R., Overview of wireless communications: Microwave perspectives, *IEEE Commun. Mag.*, (1997) 104-108.
12. Moraitis N., Constantinou P., Millimeter Wave Propagation Measurements and Characterization in an Indoor Environment for Wireless 4G Systems, *Proc. PIMRC '05* (2005).